Bulletin of the Seismological Society of America, Vol. 80, No. 2, pp. 395–410, April 1990

EARTHQUAKE LOCATIONS BY 3-D FINITE-DIFFERENCE TRAVEL TIMES

BY GLENN D. NELSON AND JOHN E. VIDALE

ABSTRACT

We present a new method for locating earthquakes in a region with arbitrarily complex three-dimensional velocity structure, called QUAKE3D. Our method searches a gridded volume and finds the global minimum travel-time residual location within the volume. Any minimization criterion may be employed. The L1 criterion, which minimizes the sum of the absolute values of travel-time residuals, is especially useful when the station coverage is sparse and is more robust than the L2 criterion (which minimizes the RMS sum) employed by most earthquake location programs. On a UNIX workstation with 8 Mbytes memory, travel-time grids of size 150 by 150 by 50 are reasonably employed, with the actual geographic coverage dependent on the grid spacing. Location precision is finer than the grid spacing. Earthquake recordings at six stations in Bear Valley are located as an example, using various layered and laterally varying velocity models. Locations with QUAKE3D are nearly identical to HYPOINVERSE locations when the same flat-layered velocity model is used. For the examples presented, the computation time per event is approximately 4 times slower than HYPOINVERSE, but the computation time for QUAKE3D is dependent only on the grid size and number of stations, and independent of the velocity model complexity.

Using QUAKE3D with a laterally varying velocity model results in locations that are physically more plausible and statistically more precise. Compared to flat-layered solutions, the earthquakes are more closely aligned with the surface fault trace, are more uniform in depth distribution, and the event and station travel-time residuals are much smaller. Hypocentral error bars computed by QUAKE3D are more realistic in that the trade-off of depth versus origin time is implicit in our error estimation, but ignored by HYPOINVERSE.

INTRODUCTION

Earthquakes have been located from travel times for more than 50 years (Lee and Stewart, 1981). Many approaches have been used, but most solve a nonlinear inverse problem. This paper will present a simple searching algorithm that is linear. Arbitrarily complex velocity models can be specified, subject only to restrictions on the maximum grid size, and therefore resolution, that are imposed by the computer memory size.

We present an example from the Bear Valley-Stone Canyon region in central California to show the usefulness of our approach. We locate earthquakes with a number of velocity models and compare the results to HYPOINVERSE solutions with a flat-layered velocity model. We then find that a laterally varying velocity model gives significantly better results than the 1-D models.

METHOD

In concept, the finite-difference scheme that we name QUAKE3D is simple. The solution proceeds in two steps. First, the travel times to all the discretized grid points in the volume that is thought to contain the earthquakes are computed from each receiver location. Second, for each set of travel times from a particular event, the location that produces the smallest travel time residual is found.

The first step, the computation of travel times, is done with the method of Vidale (1990), which is the generalization to three dimensions of the two-dimensional scheme of Vidale (1988). This method extrapolates travel time from point to point on a Cartesian grid by finite-differencing the eikonal equation of raytracing, and only records the first arrival, whether it is a geometric ray, a refraction, or a diffraction. QUAKE3D assumes the true first arrival has been picked, as do most other location programs. Since QUAKE3D can handle more complicated velocity structures than most other location programs, there is an increased risk that the first arrival calculated might not be observed. The volume around Bear Valley is gridded with 160 by 126 by 40 grid points (0.5 km spacing), so that for each station, nearly a million travel times are computed with this rapid method. In practice, we resample the travel times to a 80 by 63 by 20 point grid (1 km spacing) prior to the grid search. Once we have these travel times, every one of the grid points can be evaluated as a possible location and the travel-time residual calculated.

The location can be found using either the L1 or L2 norm criterion. The L2 norm solution will be presented first. From the set of arrival times T_{obs} and the calculated travel times T_{calc} for each of the N stations, the best fitting origin time T_{org} for a particular grid point may be found by the formula

$$T_{org} = \frac{1}{N} \sum^{N} (T_{obs} - T_{calc}).$$

Once the best origin time for the grid point has been found, the mean square travel-time residual is computed from the equation

$$R^2 = \frac{1}{N} \sum^{N} (T_{obs} - T_{calc} - T_{org})^2.$$

The grid point that has the smallest residual is considered the best location. This location is further refined by interpolation within the surrounding 3 by 3 by 3 cube of grid points. This cube is resampled to a finer grid measuring 21 by 21 by 21 grid points and a higher resolution search is made for the point with the minimum residual.

The L1 norm solution proceeds in the same fashion as L2. For each of the N stations, form the quantity $T_{org} = T_{obs} - T_{calc}$. The origin time in the L1 case is the median of the T_{org} for all the stations, rather than the average, as it was in the L2 norm case. The residual is

$$R = \frac{1}{N} \sum^{N} | T_{obs} - T_{calc} - T_{org} |.$$

Again, the grid point with the smallest residual is the best location.

The L2 norm is employed in the widely used local earthquake location programs HYPOINVERSE (Klein, 1978, 1988) and HYPO71 (Lee and Lahr, 1975). Unlike QUAKE3D, these programs and others compute not only the travel time, but also its derivatives and then use a matrix inversion to iterate toward the best hypocentral location. The L2 norm is more easily used in the matrix inversion than the L1 norm, although the L1 solution is less sensitive to outliers in the data and should result in better locations than the L2 criterion (Draper and Smith, 1981; Prugger

and Gendzwill, 1988). Because QUAKE3D is a grid searching solution, we can use L1 or L2 with equal ease. A directed grid searching algorithm that employs nonlinear inversion, but does not require computation of travel-time derivatives is described by Sambridge and Kennett (1986). The simplex searching algorithm has been employed for a somewhat similar solution to ours by Prugger and Gendzwill (1988). Their method also avoids computation of travel-time derivatives and matrix inversion. Directed searching algorithms may not find the best solution in a complex velocity model, but instead might find a local minima. Our method of computing travel times finds the global minimum travel time, rather than a ray that might be a local minimum in travel time.

A few comments about the implementation and practical aspects of running QUAKE3D are in order. QUAKE3D requires a great deal of memory for the travel-time array, on the order of 1 Mbyte per station for high resolution studies (0.5 km spacing, 100 by 100 by 25 km grid, resampled to 1 km) and 500 Kbyte for low resolution (2.5 km spacing, 400 by 400 by 100 km grid, resampled to 5 km). In the high resolution case, for precise relative locations, the number of stations need not be large, but rather the station geometry should be as constant as possible; this reduces the need for very large travel-time files. For lower resolution studies the smaller travel-time array size allows for an increase in the number of stations. The spatial extent of the grid could be extended or the memory requirements could be decreased by using variable grid spacing, but we have not implemented this feature. Execution time is linearly dependent on the grid size and number of stations. The take-off angle and azimuth can be easily found by determining the direction of maximum gradient at the hypocenter; the gradient points back to the source, which, in our method, is the receiver.

Accuracy of Method

Synthetic Data Set

We relocated synthetic events in a constant velocity half-space to test the combined effect of the real station distribution and small errors due to the finite-difference travel-time calculation. The data set consists of north-south and east-west lines of events that are centered near station BVL. We analytically computed travel times to the six Bear Valley stations used in this study, and did not apply random reading errors or station delays. The worst locations differ by less than 0.6 km horizontally and less than 0.8 km in depth along each line, and less than 1 km perpendicular to the line, as seen in Figure 1. The absolute errors are minimum at the top and center of the vertical planes and increase smoothly, but not linearly, at the bottom and far edges.

We also placed 50 events at random locations throughout the grid in a constant velocity half-space. Table 1 shows the average and maximum errors in locations, origin time, and event residuals for the L1 solutions for the random events. Errors greater than about 0.7 km occur only for events near the edges of the grid. Events near the horizontal edges are generally difficult to locate due to poor azimuthal coverage. Events near the top of the grid are poorly constrained in depth. These problems are shared with other location procedures. A problem unique to a grid searching method, such as QUAKE3D, is that an event that occurred at the bottom boundary or beyond cannot be properly located in depth. The grid depth must be chosen to not only include the deepest events, but also to contain the deepest first arrival rays. The maximum ray depth can be quickly found using a raytracing program (a number of public domain programs are available, e.g. RAYAMP by

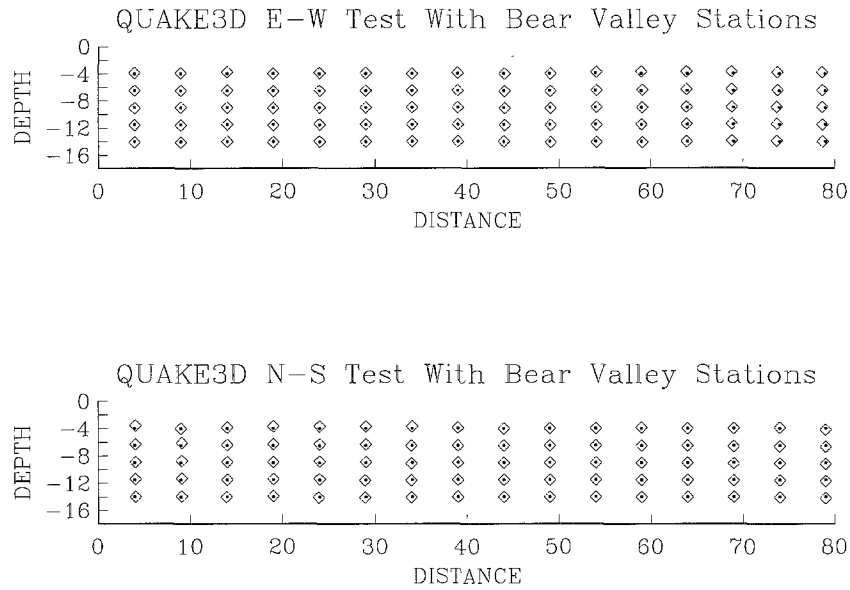

FIG. 1. Locations of strings of artificial events. Dots are the true location, diamonds the computed location from QUAKE3D. The velocity model is a homogeneous half-space, the travel-time grids were computed by finite differences. The lines cross at their centers near station BVL and extend ±40 km in each direction. Locations are in error by less than one km.

TABLE 1

SYNTHETIC DATA ERRORS

Horizontal		Depth		Origin Time		Residual	
Average	Maximum	Average	Maximum	Average	Maximum	Average	Maximum
0.172	3.77	0.31	3.00	0.033	0.66	0.0024	0.030

D. Crossley, McGill Univ.), but, as a rule, for shallow (<15 km) earthquakes, the first arrival at distances of less than 100 km usually does not penetrate to a depth greater than the Moho.

Earthquake Data Set

First arrival data was obtained from the USGS and the Seismographic Stations at University of California, Berkeley, for the time period 1977 through 1986. The USGS stations BBN, BSC, and BVL have been continuously operating during this time. The UC-Berkeley (UCB) stations LLA, PRI, PRS, and SAO have also been continuously operating during this time. We use first arrivals from only these stations in order to maintain high relative location accuracy, and for continuity with previous work by McNally and McEvilly (1977). We used the first arrival times for these stations that were redetermined by McNally and McEvilly (1977) for the time period 1975 to 1982, and are accurate to within 0.1 sec; some additional events with $M_L \geqq 2.0$ are also included in this data set. We found that first arrivals from PRI, which is by far the most distant station, consistently had the largest residual in the L1 solution and therefore we did not use this station. The six stations that we use are shown in Figure 2. Only events with all six stations reporting are relocated; with our restricted station list, this necessitates that we have first arrivals

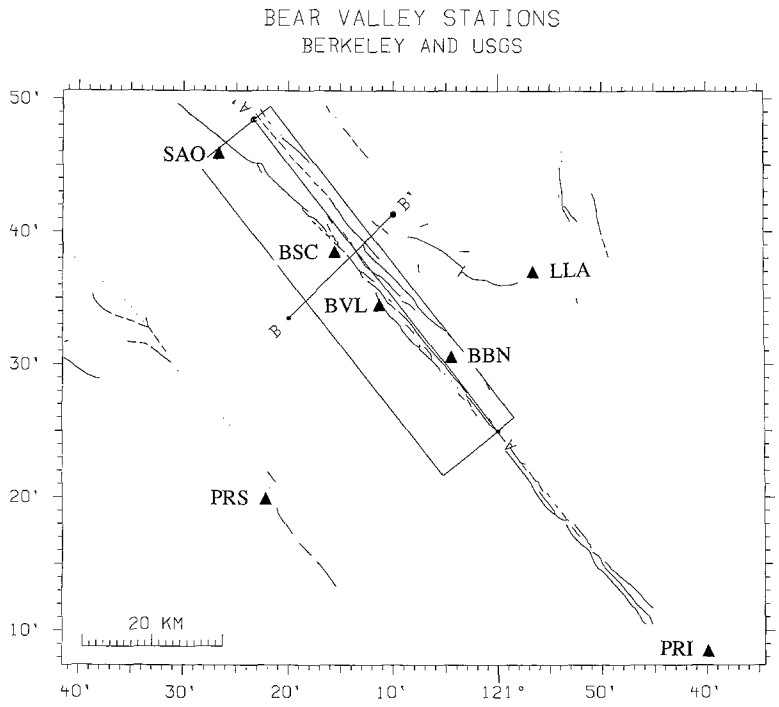

FIG. 2. Map of Bear Valley showing stations used for relocations, cross section lines for other figures, and mapped Quaternary faults from USGS. Cross sections parallel to the fault only include earthquakes within the box around line A–A′ (center line for lateral fault models). Also shown is the center point for the two lines in Figure 3.

from both the USGS and UCB. UCB generally reports only events with $M_L \geqq 2.5$ in their catalog. Since 1984 the UCB computer database reports first arrivals for some events down to $M_L \geqq 2.3$, but the published catalog is complete only to $M_L \geqq 2.5$ (E. Major, personal comm., 1988). A few of the events reported by UCB were not found in the USGS phase data and since we only use events with six stations, our relocated earthquake data set is probably complete only for $M_L > 2.5$. UCB first arrivals for 1983 are taken from the published catalog. UCB first arrivals from 1984 onward are taken from their computer data base. The UCB first arrivals from 1983 onward are accurate to 0.1 sec. USGS first arrivals for 1983 onward are taken from the original phase tapes.

Velocity Models

Lateral variations in velocity across the San Andreas in the Bear Valley–Stone Canyon region have been discussed in many studies, recently in Feng and McEvilly (1983) and Mooney and Ginzburg (1986). Boore and Hill (1973) relocated Bear Valley events by using a simple model of homogeneous half-spaces on each side of the fault, 6 km/sec to the SW and 5 km/sec to the NE. This moved locations approximately 3 km NE so that the epicenters now fell along the western edge of the San Andreas fault zone. Boore and Hill (1973) noted that station corrections with a flat-layered model could achieve nearly the same effect. Michael (1988) relocated earthquakes along the Calaveras fault, California, using a three-dimensional velocity model and also commented on the similarity to locations with a one-dimensional model with station corrections. McNally and McEvilly (1977) located

Bear Valley earthquakes using a flat-layered model with station corrections (McEvilly and Chuaqui, 1968) and arrivals from an unchanging group of seven stations, which was identical to our group plus the station PRI.

The mapped surface faults (Fig. 2) suggest a wide zone of deformation, rather than a sharp fault boundary. The reflection data of Feng and McEvilly (1983) and review by Mooney and Ginzburg (1986) both suggest a low-velocity zone approximately 3 km wide. Mooney and Ginzburg interpret prior studies to indicate up to a 30 to 45 percent decrease in velocity, but note that the average decrease is probably less. McNally and McEvilly (1977) observed anomalous first-motion directions that are consistent with a wide low-velocity fault zone, although the data are also consistent with a sharp fault with lateral velocity discontinuity across it.

According to Mooney and Ginzburg two basic models have been postulated for the gouge zone: constant velocity contrast down to the depth of 15 km or more, and a velocity contrast that decreases with depth. A model with a high contrast at the surface, exponentially decreasing with depth may give travel times that are very similar to a constant, but smaller, velocity contrast. Feng and McEvilly's (1983) data indicates that the velocity contrast fluctuates above 15 km, then decreases quickly. Michael's (1988) simultaneous inversion indicates that contrast decreases with depth, though along the fault near Morgan Hill there may be a sediment-filled valley.

We present Bear Valley earthquake relocations for one one-dimensional and two two-dimensional velocity models. These models are illustrated in Figure 3 and explained below. The first model, shown in Figure 3a, is the upper two layers from the three layer velocity structure used by McNally and McEvilly (1977). We have relocated earthquakes for this model with QUAKE3D with no station corrections and with HYPOINVERSE with and without the station corrections used by McNally.

The two-dimensional models are based on reflection data from Feng and McEvilly (1983), shown in Figure 3b, but the gouge zone is modified. Our derived velocity models for the SW and NE sides of the fault are shown in Figures 3c and d. The center of the fault zone is shown as the cross section line, A–A', on the map in Figure 2. The line is oriented to agree in azimuth with the trend of epicenters (the trend of the epicenters does not depend on the trend of the fault zone). The first two-dimensional model has a sharp boundary between the SW and NE velocity structures. The second two-dimensional model has a gouge zone centered on the cross section line; within the gouge zone the velocity at a given depth is lower than the average velocity of both sides at the same depth. We have tried models with a fixed 15 and 30 percent velocity decrease in the gouge zone, and with a velocity decrease that is greatest at the surface and decreased exponentially with depth. These variations of the gouge zone model are discussed later.

Comparison of Models by Travel-Time Residuals

Both QUAKE3D and HYPOINVERSE minimize the travel-time residual as the criterion for the best location. If the velocity model is perfect, each station should have an average residual of zero; if random errors are absent, each station would furthermore have zero standard deviation of errors. We judge the overall quality of each velocity model by a parameter which we call the model residual. The L1 model residual is the average of the absolute travel time residuals at all stations for all events. The L2 model residual is the RMS average of the travel-time residuals at all stations for all events. The L1 model residual is the appropriate measure for

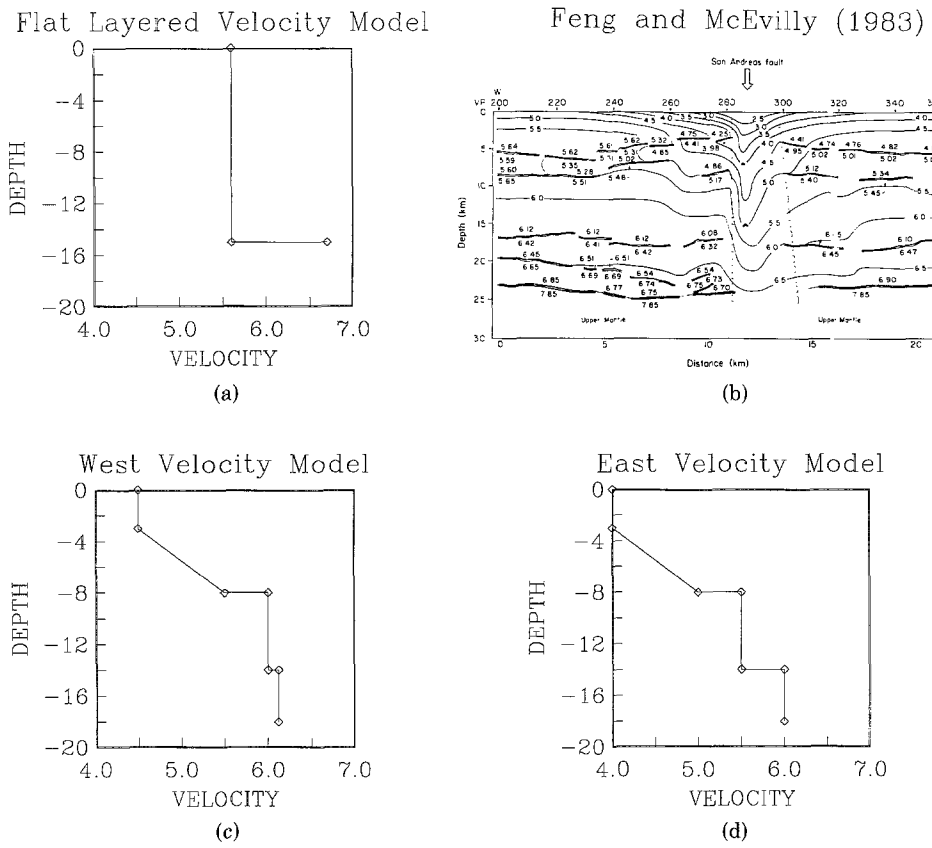

FIG. 3. Velocity models. (a) Three layer model from McNally (1975); only the first two layers are significant for first arrivals at the stations that we use. (b) Velocity cross section from reflection line of Feng and McEvilly (1983). (c) West of fault velocity model derived from Feng and McEvilly. (d) East of fault velocity model derived from Feng and McEvilly.

locations found using L1 minimization, and the L2 model residual is appropriate for L2 minimization (the appropriate numbers are boldface in Table 2). Both L1 and L2 measures of the model residual are summarized in Table 2. The parameters in Table 2 are computed only from events that were reported at all six stations (161 events). In addition, we exclude events of depth $\geqq$13 km, because they had high residuals and mostly were computed to be at the bottom grid boundary; this restriction excludes only between 4 to 7 events, depending on the model. Station delays were not used unless indicated in the table. The models and methods are ranked by the model residual from best to worst.

The gouge zone model is the best, followed by the sharp and two flat models among the locations computed by QUAKE3D. The best gouge zone model, partly based on the discussion in Mooney and Ginzburg (1986) and Michael (1988), has a 30 percent velocity decrease in the gouge zone, at the surface, with the contrast decreasing with depth as $e^{-Z/8}$ (in km). A gouge zone model with 15 percent constant velocity contrast is only 8 percent worse. (The two other related models, 30 percent constant and 15 percent exponential, were not nearly as good: residual = 0.061 and 0.039, respectively). Application of station delays to the best gouge zone model resulted in a further 17 percent improvement in model residual (station delays are discussed later). Since HYPOINVERSE uses an L2 solution, we compare with

TABLE 2
MODEL RESIDUALS (SECONDS)

Program	Model	Location Criterion	L1 Res	L2 Res	Max Event Res
QUAKE3D	Gouge Sta Delay	L1	**0.028**	0.062	0.16
	Gouge No Delays	L1	**0.033**	0.075	0.17
	Gouge Sta Delay	L2	0.040	**0.059**	0.22
	Sharp	L1	**0.049**	0.098	0.21
	Sharp	L2	0.061	**0.083**	0.36
	Flat	L1	**0.053**	0.111	0.23
	Flat	L2	0.065	**0.093**	0.39
	EW Avg	L1	**0.054**	0.114	0.18
	EW Avg	L2	0.069	**0.094**	0.33
HYPO	Flat No Delays	L2	0.063	**0.087**	0.40
	Flat Sta Delays	L2	0.068	**0.092**	0.37

QUAKE3D L2 model residuals. The HYPOINVERSE model residual with no station delays has slightly smaller residuals than QUAKE3D with a flat velocity model, and the difference (1/200 sec) is due to small errors in the travel-time calculation. Surprisingly, the HYPOINVERSE solution with no station corrections has a smaller model residual than the solution with corrections, despite the fact that the station corrections move the epicenters closer to the gouge zone model locations (this is discussed and illustrated below). The worst model used a flat velocity structure that is the average of the east and west sides of the 3-D model that we used in the gouge and sharp cases. For this model, epicenters were similar to the other flat model, but deeper because the velocities are higher.

Comparison of L1 and L2

For the gouge model we can compare the L1 and L2 locations. The L1 locations have a better L1 model residual than the L2 locations do and, conversely, the L2 locations have a better L2 model residual than the L1 locations, which is expected. The epicentral locations are nearly all the same and are not shown. The depths are also nearly all the same, as seen in the two cross sections in Figure 4. For those few events that are different, we found that one or more stations had a large residual; thus the locations differ because the L1 solution is less sensitive to outliers than the L2 solution. This data is very carefully picked, so typical data might have greater reading errors and benefit more from the L1 solution.

Comparison of Bear Valley Locations

We have relocated earthquakes in Bear Valley that occurred from 1977 through 1986, using only events that were reported by all six stations BBN, BSC, BVL, LLA, PRS, and SAO. The long tenure of these nearby stations allows a consistent set of arrivals for many years (McNally and McEvilly, 1977).

Figures 5 through 9 show relocations of 53 events, selected to be distributed across the study area, using both QUAKE3D and HYPOINVERSE (indicated by dots and squares, respectively). The QUAKE3D locations are from our best model,

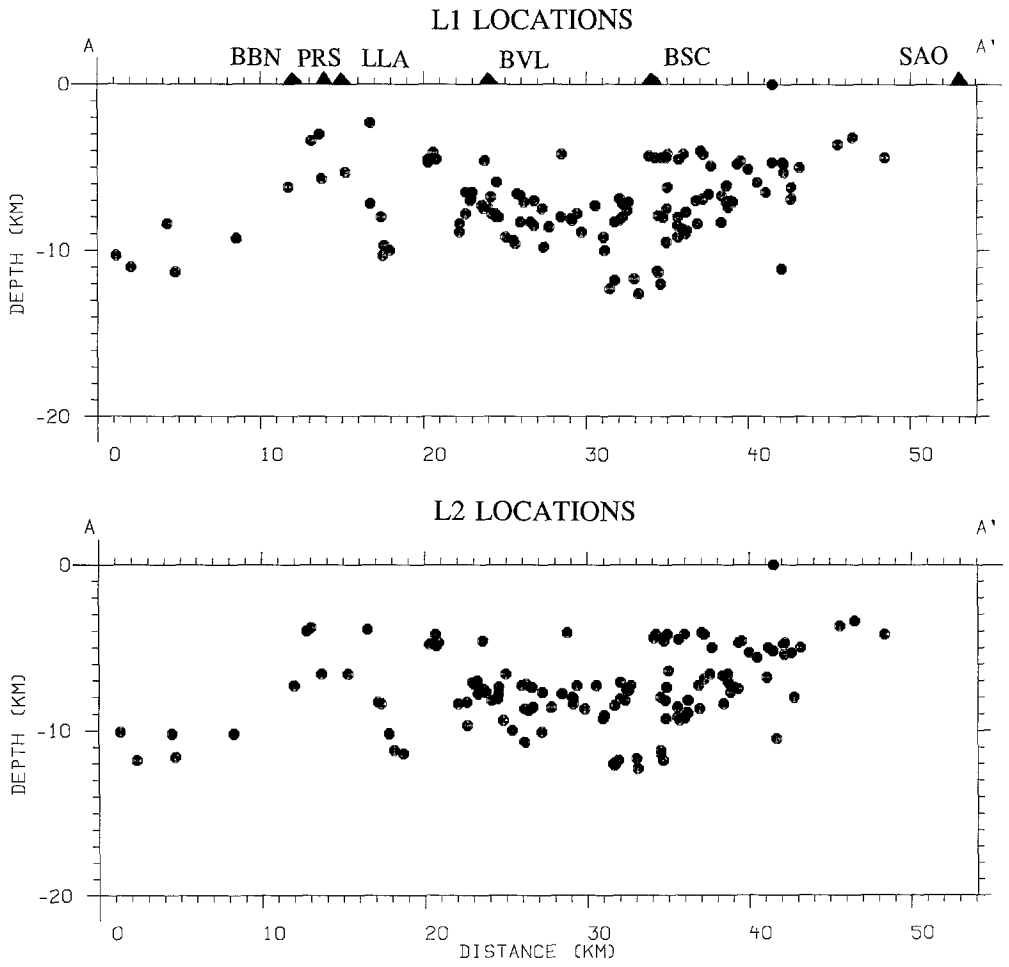

FIG. 4. Cross section along A–A′ of all events within box (see Fig. 2) as determined by L1 and L2 criterion.

a 3-km-wide fault zone with velocity 30 percent lower in the fault zone at the surface and contrast decreasing exponentially with depth as $e^{-Z/8}$ (where Z is depth in km), and lower velocities to the NE than to the SW of the fault (see Figs. 3c and d). The HYPOINVERSE locations use the one-dimensional velocity model shown in Figure 3a. The figures show a map view and cross sections parallel and perpendicular to the San Andreas fault (cross section lines are shown in Fig. 2). The cross section figures along strike include only earthquakes in the box shown in Figure 2. The surface fault trace bends to the west in Bear Valley, so the cross section line is not always parallel to the fault. The *A–A′* line, parallel to the fault trace, also marks the fault boundary for the three-dimensional models. We have found that the epicenters are insensitive to the precise location of this dividing line with the laterally varying models, but the average station residuals are strongly affected by being on one side of the fault boundary or the other.

The map view of seismicity (Fig. 5) shows more sensible locations when a three-dimensional velocity model is employed. The earthquakes lie close to the western-most mapped fault trace, whereas the one-dimensional locations without station delays lie an average of 3 km SW of the fault and bend away to the NW. The USGS

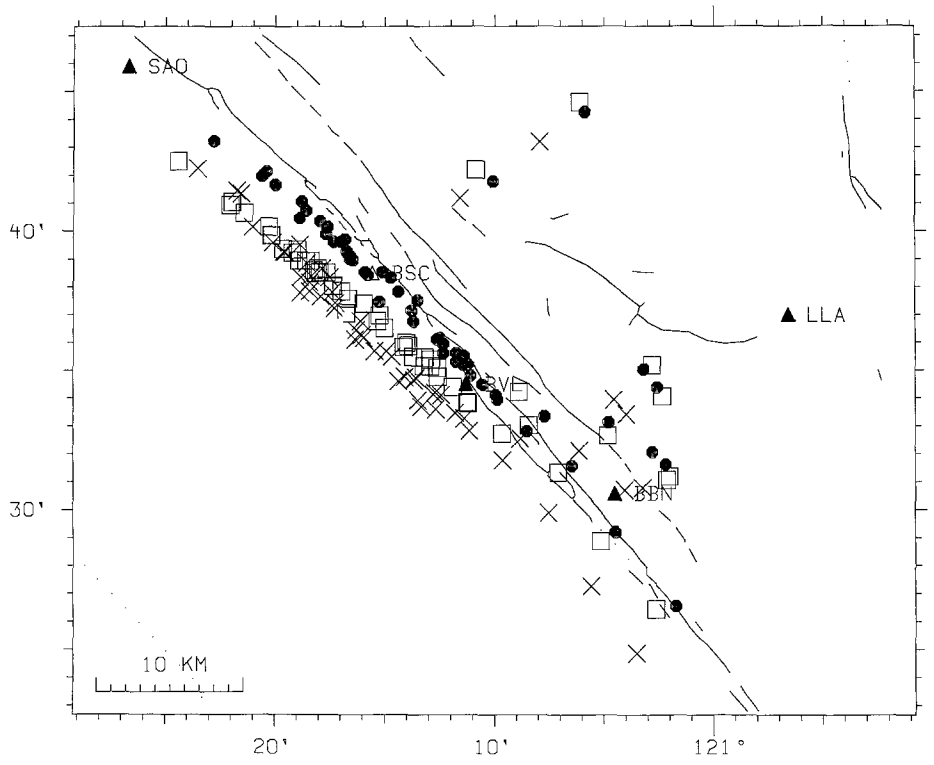

FIG. 5. Map view comparing our best locations, using the gouge zone model, with HYPOINVERSE using the flat velocity model with no station corrections, and with USGS Calnet locations. Solid circles for gouge zone locations, squares for HYPOINVERSE, crosses for Calnet. The earthquakes are 54 events selected from 1977 to 1986. The gouge model places the earthquakes close to the westernmost mapped fault trace, but the uncorrected flat-layered locations lie a few km to the southwest. The Calnet locations are generally further from the fault than the flat-layer solutions.

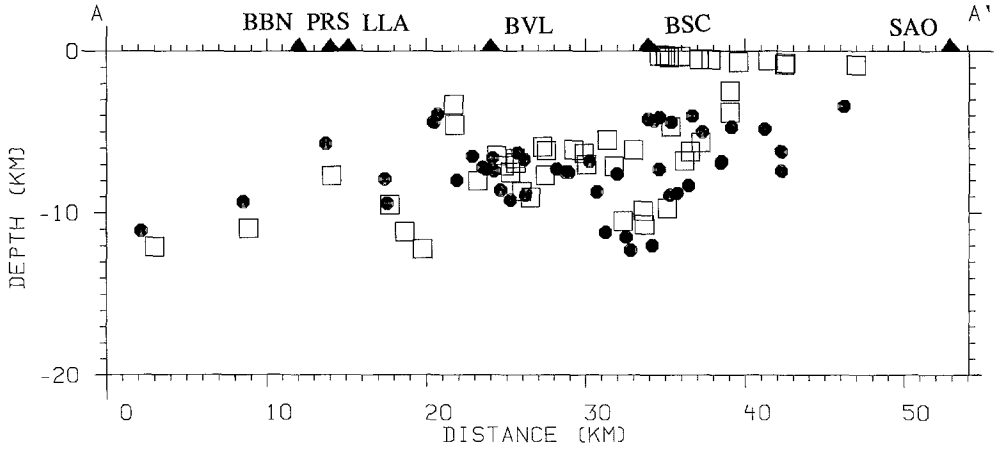

FIG. 6. Cross section along line A–A′ (parallel to fault, Fig. 2) as in Figure 5, but not showing Calnet locations. QUAKE3D with the gouge zone model gives deeper locations than HYPOINVERSE with the flat model from 20 to 50 km, and has no near-surface events, which are probably in error.

Calnet locations, which use more stations and a different velocity model, are also shown and lie even further to the SW than our flat-layered solutions. The parallel cross section (Fig. 6) shows that the three-dimensional locations are consistently deeper than the one-dimensional locations. Many of the northern events are located

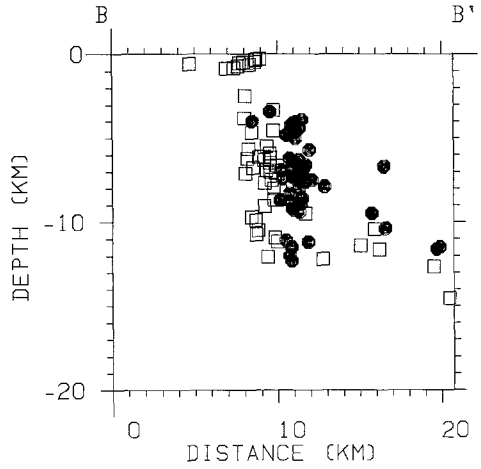

FIG. 7. Cross section along line B–B′ (perpendicular to fault, Fig. 2) as in Figure 5.

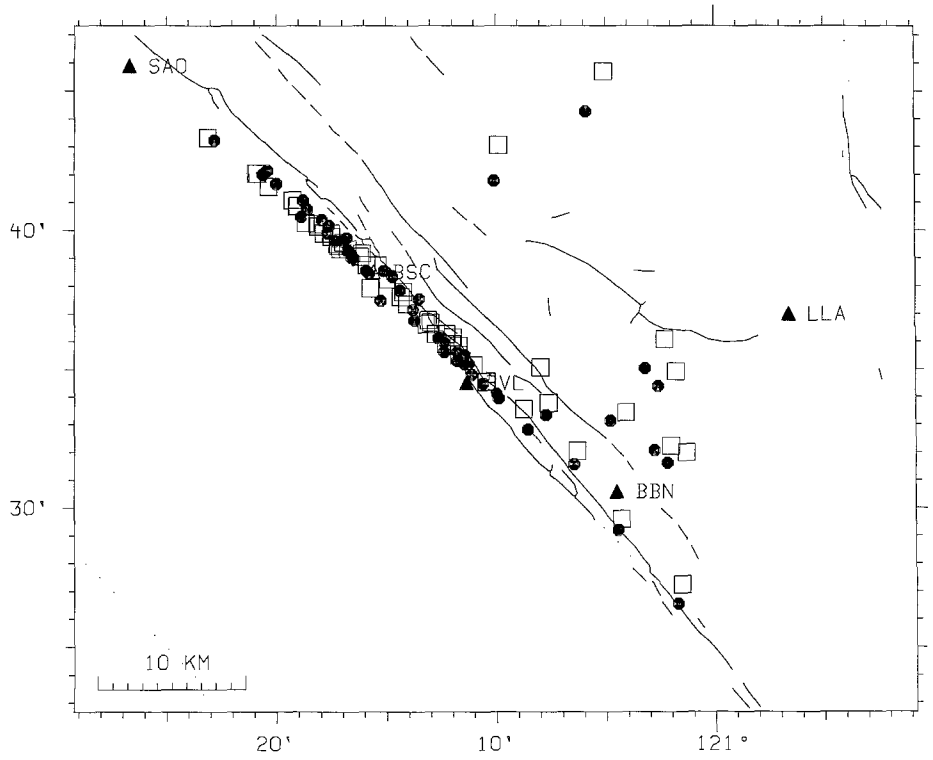

FIG. 8. Map view comparing our best locations, using the gouge zone model, with HYPOINVERSE using the flat velocity model with station corrections at LLA and PRS. Unlike Figure 5, these epicentral locations are very similar.

less than 1 km deep in the one-dimensional locations. The perpendicular cross section (Fig. 7) shows both the greater average depth and the lesser offset relative to the mapped fault trace. In Figure 7 the greater spread of the one-dimensional locations is due to the fact that their trend deviates from the azimuth of the cross section line, not due to greater scatter in their relative locations.

Location error estimates are determined from the 21 by 21 by 21 travel-time residual fine grid. The travel-time error estimate is just the travel-time residual. To

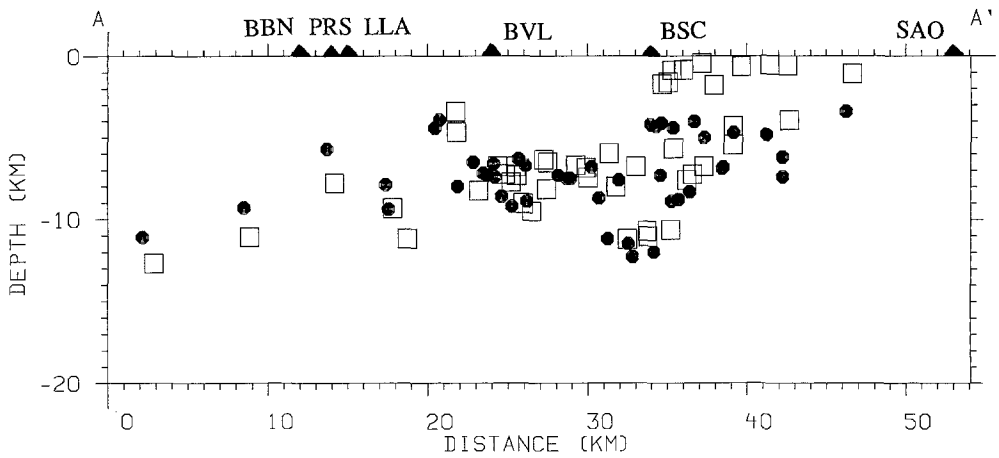

FIG. 9. Cross section along line A–A′ (parallel to fault, Fig. 2) as in Figure 8. The station corrections move the HYPOINVERSE locations deeper, but cannot eliminate the near surface events.

estimate the spatial errors, we fit a curve to the 21 travel-time residuals in each direction (xyz) and compute the distance at which the residual increases by one standard deviation. For L1 estimates, the residuals increase linearly away from the minimum, so we actually fit two straight lines, then average the error estimates. For L2 estimates we use a parabolic fit. For a least squares solution, the value of the travel-time residual at one standard deviation is estimated to be $(N + 1)\sigma/N$, where N is the number of degrees of freedom (number of stations: 1) and σ is the standard deviation of the travel time (RMS residual) (John Haines, personal comm., 1989). We found that using this estimation of the error for the L1 solution gave errors that were smaller than HYPOINVERSE, but that estimating the errors at 2σ gave results that were comparable. Our method of estimating the location errors implicitly includes the tradeoff of depth versus origin time, whereas HYPOINVERSE uses a fixed origin time and therefore incorrectly underestimates the spatial location errors. QUAKE3D generally computed depth errors that were greater than HYPOINVERSE when the travel-time residuals were high, even though the horizontal errors remained comparable, which is the expected behavior. The calculated errors are a combination of relative errors due to timing error, and absolute errors due to the velocity model. Although our velocity model produces small residuals, it is difficult to estimate the magnitude of the absolute errors. The average horizontal and depth errors computed by QUAKE3D are 0.6 and 1.4 km, respectively, for the events shown in Figures 5 to 7. We have not shown error bars because the errors are comparable to the symbol size.

We also used McEvilly and Chuaqui's (1968) station corrections with HYPOINVERSE. These corrections are −0.3 sec for LLA to the NE (slow velocity) and +0.3 sec for PRS to the SW (fast velocity), independent of event location. The HYPOINVERSE locations with station delay corrections are compared to our L1 gouge model locations in Figures 8 and 9. The map view in Figure 8 shows that the epicenters for these two models are now close to each other, however the gouge model locations tend to be slightly closer to the mapped fault at all latitudes. This is sensible for the linear trend of events that were previously mapped to the SW of the fault, but we cannot say what we expect for the events that exhibit no trend and may be truly located within the gouge zone, or to the NE of the fault zone. The

cross section parallel to the fault zone is shown in Figure 9. The gouge zone locations are generally deeper than HYPOINVERSE with station corrections. The shallow depths found by HYPOINVERSE to the NW (near A') do not occur in the QUAKE3D locations. The shallow depths are probably not realistic. McNally and Bryant's locations (personal comm., 1988), using PRI plus fine station corrections, have fewer shallow earthquakes than our HYPOINVERSE locations, but more than the gouge zone locations.

Station Corrections

We were able to improve the model residual for the best gouge zone case (30 percent contrast, exponential decrease) by applying station corrections. Station corrections are a simple method of compensating for unknown velocity structure along the path from the average event hypocenters to each station. If the hypocenters are broadly distributed about the station, the station correction is largely due to near station (shallow) velocity structure. To compute the correction, the station residuals for all events are averaged and subtracted from the arrival times. The maximum station correction was −0.06 sec at station LLA. The new hypocenters were on average within 0.3 km of the hypocenters without corrections and the model residual improved by 11 percent. We were able to improve the model residual in a second pass by an additional 6 percent by further adjusting the station corrections from the first pass.

Discussion and Conclusions

Figures 10 through 12 show the locations of all 161 events recorded by all six stations between 1977 and 1986. We can evaluate the correctness of locations by the quantitative criterion of (model) residual and by the qualitative criterion of proximity to known faults. Judged by the model residual, the best models use differing east and west velocities, but the worst model uses the average of those velocities; this model is also not nearly as good as the simple two-layer flat model derived from McNally and McEvilly (1977), even though the epicenters are similar. The greatest improvement in model residual is therefore attributable to using a laterally varying velocity model, and not to the choice of velocity as a function of depth. Judged by the alignment of epicenters with the mapped fault trace, the best velocity model is one that has differing structure on each side of the fault. A significant, but smaller, improvement in model residual results when the gouge zone velocity contrast decreases with depth, rather than remaining constant. Such a gouge zone model is probably more realistic than a fixed contrast with depth, and agrees with data of Feng and McEvilly (1983) and results of Michael (1988) and Cormier and Beroza (1987).

All of the laterally varying velocity models (with or without gouge zone) with no station corrections give similar locations that are significantly different from the flat-layered models without station corrections. The average hypocenter depth is greater and depths are almost exclusively in the range of 4 to 12 km, whereas there is a greater spread of depths for the flat-layered model. This observation of no shallow seismicity should be considered more accurate than previous locations in this region, although absolute errors are difficult to estimate. The earthquake epicenters are aligned along the westernmost mapped surface trace, but deviate slightly westward to the NW (see Fig. 8). These observations imply that we could obtain better alignment to the NW by also varying the velocity model along the strike of the San Andreas. McNally and McEvilly (1977) additionally used station

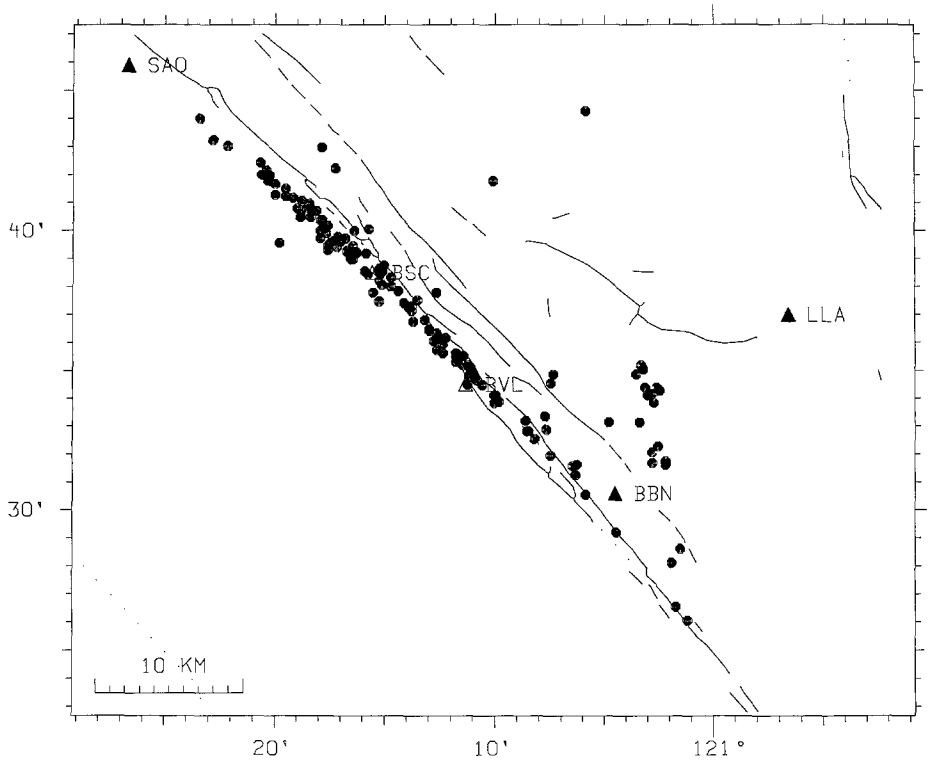

FIG. 10. Map view of 221 earthquakes from 1977 to 1986, $M_L \geqq 2.5$ as located by the gouge model with QUAKE3D.

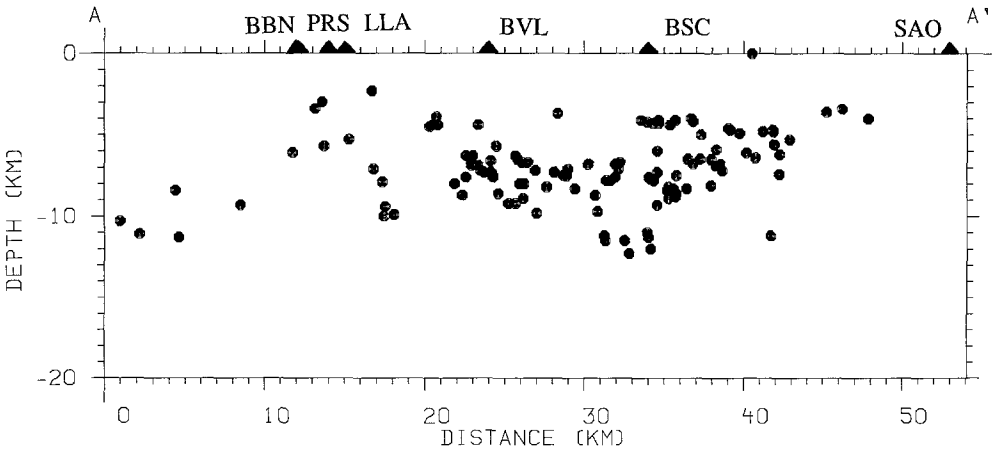

FIG. 11. Cross section along line A–A′ (Fig. 2) of earthquakes in Figure 10.

corrections that varied with the latitude of the epicenter, which are consistent with velocity variations along strike. The USGS Calnet also uses some large station corrections (+0.26 sec at BBN), but their station corrections and velocity model are derived for a much larger region; the result is that epicenters are located about 3 km SW of the fault trace. Due to the use of a laterally varying velocity model, we were able to obtain better locations than with a flat-layered model, without using

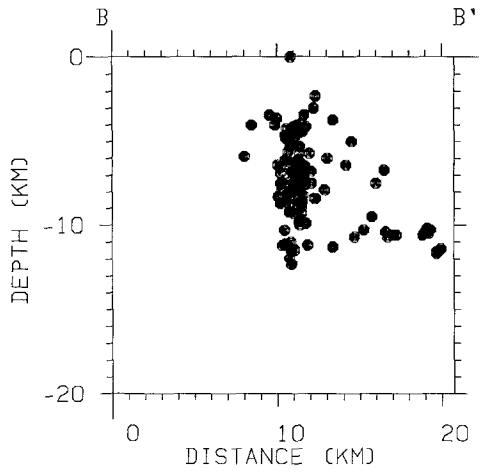

FIG. 12. Cross section along line B–B′ (Fig. 2) of earthquakes in Figure 10.

station corrections. We determined station corrections (maximum 0.06 sec) and were able to improve event residuals, but saw almost no change in hypocentral locations.

QUAKE3D always finds the location with the global travel-time minimum, unlike traditional location programs. This is an important feature of our method when the medium has strong lateral variations, but has the disadvantage of generally requiring more computer time than iterative search methods. Another advantage of QUAKE3D, especially when the station distribution is poor or sparse, is the ability to evaluate locations by L1, rather than L2 norm. Inverse location programs such as HYPOINVERSE, HYPO71, and others compute the L2 residual, which is more adversely influenced by outliers. Forward searching algorithms such as QUAKE3D, the simplex method of Prugger and Gendzwill (1988), and the L1 scheme of English *et al.* (1988), benefit by being able to use any criterion for the best location. Finally, and most importantly, QUAKE3D can locate earthquakes in the presence of strong, three-dimensional velocity heterogeneities.

ACKNOWLEDGMENTS

Support for this work has been provided in part by Institute of Geophysics and Planetary Physics grant 88–37, a grant from the W.M. Keck Foundation, National Science Foundation grant EAR-8708034, and the Institute of Tectonics, University of California, Santa Cruz. We wish to thank Karen McNally for focusing our interests on Bear Valley. We also wish to thank Rick Lester of the USGS for help in obtaining Calnet data, and Fred Klein of the USGS for his unceasing efforts to keep HYPOINVERSE and QPLOT updated. Finally we thank Andy Michaels and Dave Boore for thorough reviews that improved the manuscript. Contribution number 79 from the Charles F. Richter Seismological Laboratory at the University of California, Santa Cruz.

REFERENCES

Boore, D. M. and D. P. Hill (1973). Wave propagation characteristics in the vicinity of the San Andreas fault, *Proceedings of the Conference on Tectonic Problems of the San Andreas Fault System* **XIII,** Stanford University, California, 215–224.

Cormier, V. F. and G. C. Beroza (1987). Calculation of strong ground motion due to an extended source in a laterally varying structure, *Bull. Seism. Soc. Am.* **77,** 1–13.

Draper, N. R. and H. Smith (1981). *Applied Regression Analysis*, Wiley, New York.

English, T. T., C. E. Johnson, R. Y. Koyanagi, and A. Largo (1988). Automated real-time systems for managing volcanic and seismic crises at the USGS Hawaiian Volcano Observatory, *Seism. Res. Lett.* **59,** 37.

Feng, R. and T. V. McEvilly (1983). Interpretation of seismic reflection profiling data for the structure of the San Andreas fault zone, *Bull. Seism. Soc. Am.* **73,** 1701–1720.

Klein, F. W. (1978). Hypocenter location program—HYPOINVERSE: users guide to versions 1, 2, 3, and 4, *U. S. Geol. Surv. Open-File Rept. 78–694*, 1–113.

Klein, F. W. (1988). User's guide to HYPOINVERSE, a program for VAX computers to solve for earthquake locations, *U. S. Geol. Surv. Open-File Rept. 88.*

Lee, W. H. K. and J. C. Lahr (1975). HYP071 (revised): a computer program for determining hypocenter, magnitude, and first motion pattern of local earthquakes, *U. S. Geol. Surv. Open-File Rept. 75–311*, 1–116.

Lee, W. H. K. and S. Stewart (1981). *Principles of Microearthquake Networks*, Academic Press, New York.

McEvilly, T. and L. Chuaqui (1968). Detailed crustal structure within array, The Central California large-scale seismic array, Annual Report, Jan 1-Dec 31, Seismographic Stations, University of California, Berkeley, 14–16 pp.

McNally, K. C. and McEvilly, T. V. (1977). Velocity contrast across the San Andreas fault in central California: small-scale variations from *P*-wave nodal plane distributions, *Bull. Seism. Soc. Am.* **67,** 1565–1576.

Michael, A. J. (1988). Effects of three-dimensional velocity structure on the seismicity of the 1984 Morgan Hill, California, aftershock sequence, *Bull. Seism. Soc. Am.* **78,** 1199–1221.

Mooney, W. D. and A. Ginzburg (1986). Seismic measurements of the internal properties of fault zones, *Pageoph.* **124,** 141–157.

Prugger, A. F. and D. J. Gendzwill (1988). Microcarthquake location: a nonlinear approach that makes use of a simplex stepping procedure, *Bull. Seism. Soc. Am.* **78**, 799–815.

Sambridge, M. S. and B. L. N. Kennett (1986). A novel method of hypocentre location, *Geophys. J. R. Astr. Soc.* **87,** 679–697.

Vidale, J. E. (1988). Finite-difference calculation of travel times, *Bull. Seism. Soc. Am.* **78,** 2062–2076.

Vidale, J. E. (1990). Finite-difference calculation of travel time in 3D, *Geophysics* (in press).

C. F. Richter Seismology Laboratory
University of California
Santa Cruz, California 95064

Manuscript received 18 August 1989